X-726-74-213

PREPRINT

NASA TM X- 70723

ANALYSIS OF THE VERTICAL TEMPERATURE PROFILE RADIOMETER (VTPR) RADIOMETRIC PROBLEM

I. L. GOLDBERG

(NASA-TM-X-70723) ANALYSIS OF THE VERTICAL TEMPERATURE PROFILE RADIOMETER (VTPR) RADIOMETRIC PROBLEM Final Report, 19 Jun. 1972 - 19 Jun. 1973 (NASA) 47 p HC $5.50 CSCL 14B

N74-31913

Unclas G3/14 46669

JULY 1974

GSFC

GODDARD SPACE FLIGHT CENTER

GREENBELT, MARYLAND

X-726-74-213

ANALYSIS OF THE VERTICAL TEMPERATURE PROFILE RADIOMETER (VTPR) RADIOMETRIC PROBLEM

I. L. Goldberg

July 1974

GODDARD SPACE FLIGHT CENTER

Greenbelt, Maryland

ANALYSIS OF THE VERTICAL TEMPERATURE PROFILE RADIOMETER (VTPR) RADIOMETRIC PROBLEM

I. L. Goldberg

ABSTRACT

The VTPR instruments that are presently in orbit exhibit a significant variation in bias radiation on the detector as a function of scan mirror position. Tests in the laboratory show that this bias radiation disappears when optical baffles are added. A detailed analysis explains quantitatively the observed bias variation with is due to (1) the extraneous field-of-view of the detector and (2) the variation in magnitude of the far field-of-view solid angle as a function of mirror position.

CONTENTS

APPENDIXES

ILLUSTRATIONS

PRECEDING PAGE BLANK NOT FILMED

ILLUSTRATIONS (Cont'd.)

TABLES

ANALYSIS OF THE VERTICAL TEMPERATURE PROFILE RADIOMETER (VTPR) RADIOMETRIC PROBLEM

INTRODUCTION AND SUMMARY

The VTPR telescopes that are presently in orbit (as of July 1974) do not contain optical baffles. Without baffles there is a significant variation in bias radiation on the detector as a function of scan mirror position. This is true even when the entire external scene is cold space. When scanning space the largest signal output occurs at or near scan step 10 and the smallest signal occurs near step 23. At first, it was believed that the varying bias was due to temperature gradients within the VTPR and parts of the spacecraft toward the front of the VTPR. The explanation of the varying bias is as follows:

a. The detector has an extraneous solid angle field-of-view (FOV) much larger than the nominal 2.1° x 2.1° FOV (0.00134 steradians). Recent tests indicate that the total extraneous FOV is about three orders of magnitude higher than the nominal solid angle FOV. Not all of the total extraneous FOV plays a significant role in the bias variation. Only that portion that represents the scene beyond the spacecraft causes the error. Calculations show that this portion is larger than the nominal solid angle FOV by a factor of 30 to 82, depending on scan mirror position. Although the signals from points within the extraneous field is greatly attenuated the large field size produces an appreciable radiant input.

b. When no baffles are employed, the rotation and displacement of the scan mirror changes the detector's extraneous view of the outside world. This happens because the detector can view parts of the scan mirror directly, even though a large portion is obscured by the secondary mirror. In addition, a portion of the outside scene, as viewed by direct reflection from the scan mirror, is obstructed by the VTPR housing and "race track" shaped port in front of the instrument. We shall refer to this unobstructed outside scene as the "far field" scene. As the scan mirror steps from position 1 to 23 the far field solid angle varies considerably. It is primarily this variation that causes the bias to change as a function of scan mirror position! Quantitatively, this is confirmed by the fact that the far field solid angle is greatest at step 10 and least at step 23 (see Figures 2 through 7). Thus when scanning space the largest far field solid angle will produce the least radiant input to the detector (the extraneous radiant input comes solely from the near field when the instrument scans space). Plots made by RCA AED of the far and near fields of the VTPR detector for 6 scan step positions show that there is excellent qualitative correlation between the far field solid angle and observed signal amplitude when the radiometer scans space. This is true for the instruments in orbit and those tested in the laboratory.

A quantitative analysis has been made using test data taken at Barnes Engineering with VTPR S/N 007. When baffles are installed the bias variation essentially disappears. Without baffles the bias variation was calculated using:

1. FOV measurements over a 60° x 42° field.

2. Calculated geometric FOV taken from RCA plots for 6 scan mirror positions of the VTPR.

3. Correction factors due to the out-of-focus condition in the test configuration.

Calculations were made for 6 scan mirror positions. Scan step 23 was used as a reference to obtain differences in signals. The calculated values were compared with the S/N 007 measurements for the 833 cm^{-1} channel, without baffle, and the results are shown in Figure 1. The bias radiation tests were made at Barnes Engineering with a "cold space" target at a temperature of about 100 K. The actual value of the maximum signal for the two tests shown was 837 digital counts (average). Note that only differences (ΔC) are plotted, scan step 23 being used as the reference. Considering the sensitivity of the calculations to small errors and the fact that the 1000°C source used for the FOV tests has a temperature drift of ±30°C the correlation between measured and calculated values is excellent.

DETAILED ANALYSIS

Calculations Summary

The calculated bias voltage variations can be converted to equivalent digital count variations ΔC by

$$\frac{\Delta C}{C_p} = \frac{L}{V_p} (A_n V_n - A_{23} V_{23})$$

where

C_p = peak value in digital counts, measured with VTPR S/N 007 in the 833 cm^{-1} channel in the bias radiation tests

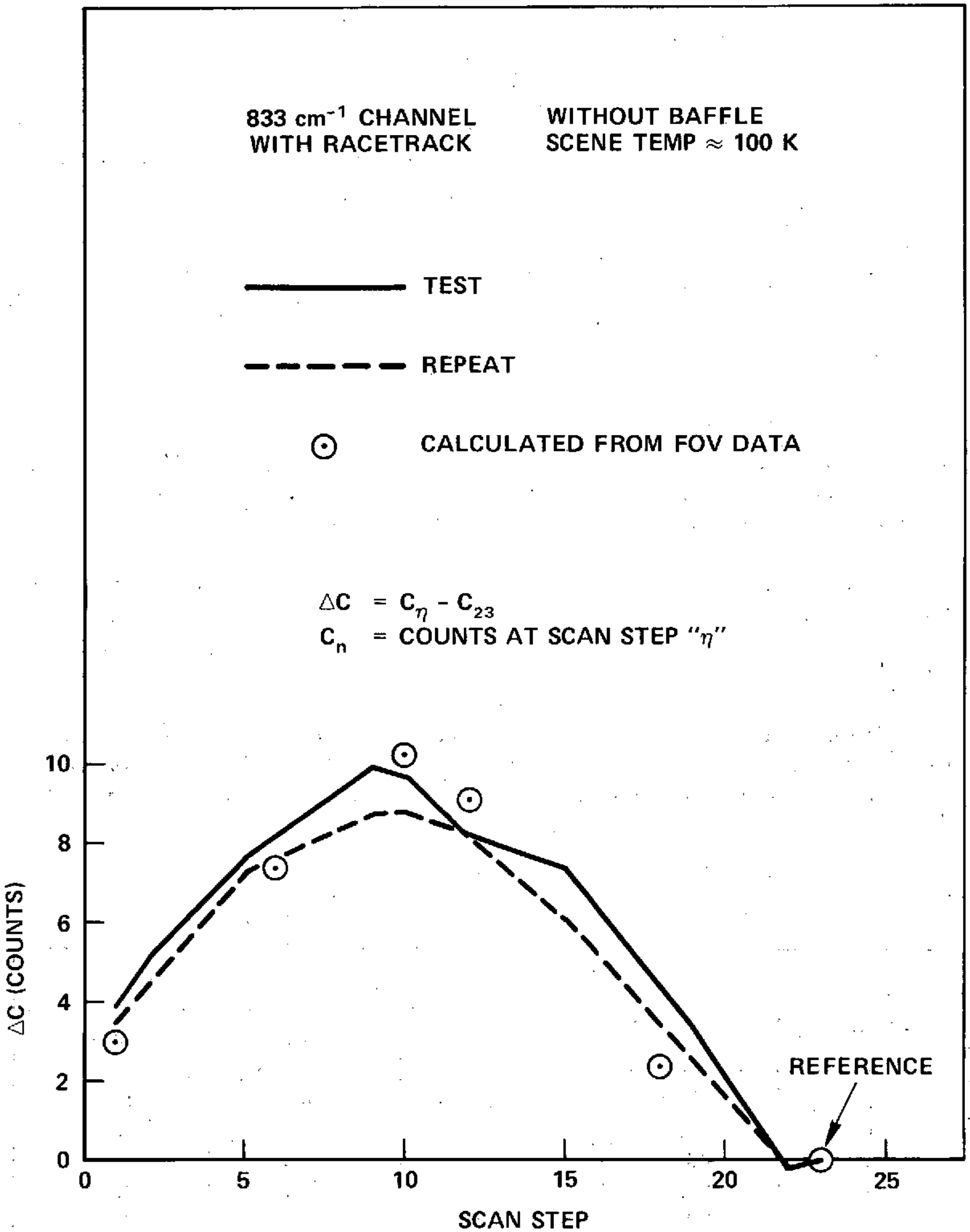

Figure 1. VTPR S/N 007 Bias Variation

L = correction factor due to out-of-focus condition during FOV tests

V_p = on-axis peak signal voltage

A_n = number of 3° x 3° elements in the far field scene for scan position n

A_{23} = number of 3° x 3° elements in the far field scene for scan position 23

V_n = average voltage within A_n

V_{23} = average voltage within A_{23}

As explained below, C_p = 837 counts, L = 0.603 and V_p = 26.0 volts. Therefore,

$$\Delta C = 0.0194\,(A_n V_n - A_{23} V_{23})$$

where V_n and V_{23} are in millivolts. The values of A_n, V_n and ΔC are shown in Table 1. The measured values of ΔC shown in the table are the average readings from the two FOV tests with VTPR S/N 007 for the 833 cm^{-1} channel.

The field-of-view tests and the method by which V_n was calculated is described in the next section.

FOV Tests

The FOV tests were made using a 2-inch diameter, 1000°C blackbody source with a radiation chopper in front of the source. The internal chopper of the VTPR was not used. The signals were taken from a test point before the A/D

Table 1

Calculated Bias Variations (833 cm^{-1} Channel)

Scan Step	A_n	V_n (mV)	ΔC (Counts)	
			Calc	Meas
1	22.2	26.5	3.0	3.6
6	33.5	24.4	7.4	7.9
10	39.6	24.3	10.2	9.3
12	35.5	25.4	9.1	8.1
18	20.0	28.0	2.4	3.9
23	14.4	30.2	0	0

converter and therefore the measured values are in volts rather than digital counts. For the extraneous FOV measurements an amplifier with a gain of 10 was employed. This external amplifier was not used for the on-axis peak signal measurement. All FOV data described in this report take amplifier gain into account.

The FOV was measured over a 60° x 42° field at 3° intervals. The peak radiation signal, collected by the primary mirror at the center of the FOV was 26 volts. The average value of the extraneous signals within the far field scene varied from 24.3 mV for scan step 10 to 30.2 mV for scan step 23. These values are "above noise" voltages, i.e., the noise voltage was subtracted from the actual voltage reading for each point measured. This is important to do since we are interested in differences only. For example, if this were not done and if there were no extraneous signals, i.e., only noise, the calculations would indicate an erroneous bias variation because the far field areas are different for different scan mirror positions. This is because the calculated bias variation is proportional to

$$A_n V_n - A_{23} V_{23}$$

So that if

$$V_n = V_{23} = \text{noise voltage} = V_N,$$

the calculated variation would be proportional to

$$V_N (A_n - A_{23})$$

This is obviously wrong. The explanation is that no account has been taken of the total field, in which all points have a value V_N. Since the total field (near and far fields) does not vary (it is always 2π steradians) the bias would not change with mirror position. Therefore, in order to eliminate this source of error in the calculations, the noise voltage has been subtracted out.

Earlier FOV tests contained erroneous measurements of the peak voltage because the amplifier used had saturated. The proper value of V_p was measured during tests run on June 12, 1974 and is 26.0 volts.

The far field views for scan steps 1, 6, 10, 12, 18 and 23 are shown in Figures 2 through 7. They are simplified versions of RCA plots of the calculated geometric FOV of the VTPR. The signal voltage readings within the usable portions of the far field views for each of the above scan mirror positions are shown in Tables 2 through 7. The first entry in each 3° x 3° box element is the relative

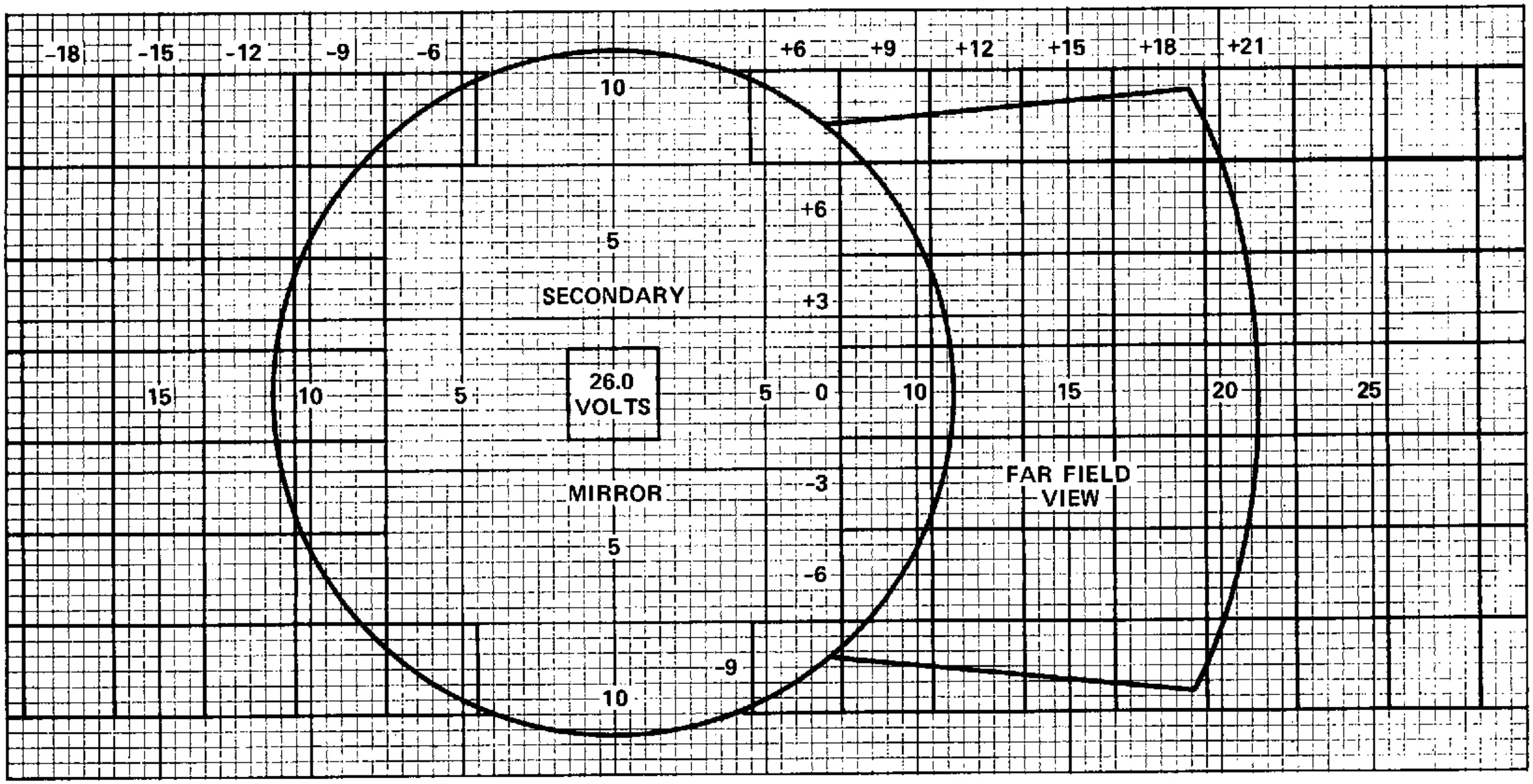

Figure 2. Scan Step 1

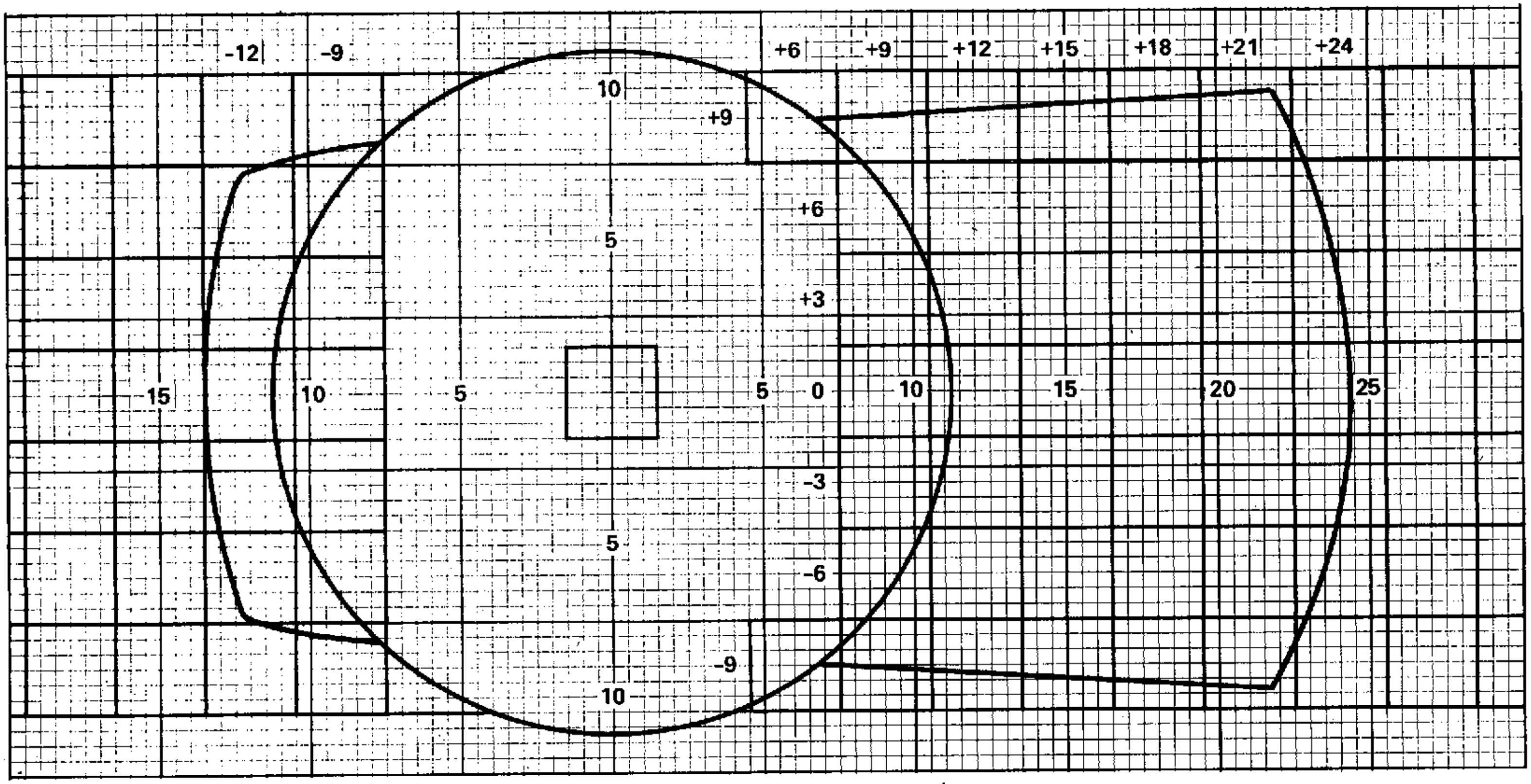

Figure 3. Scan Step 6

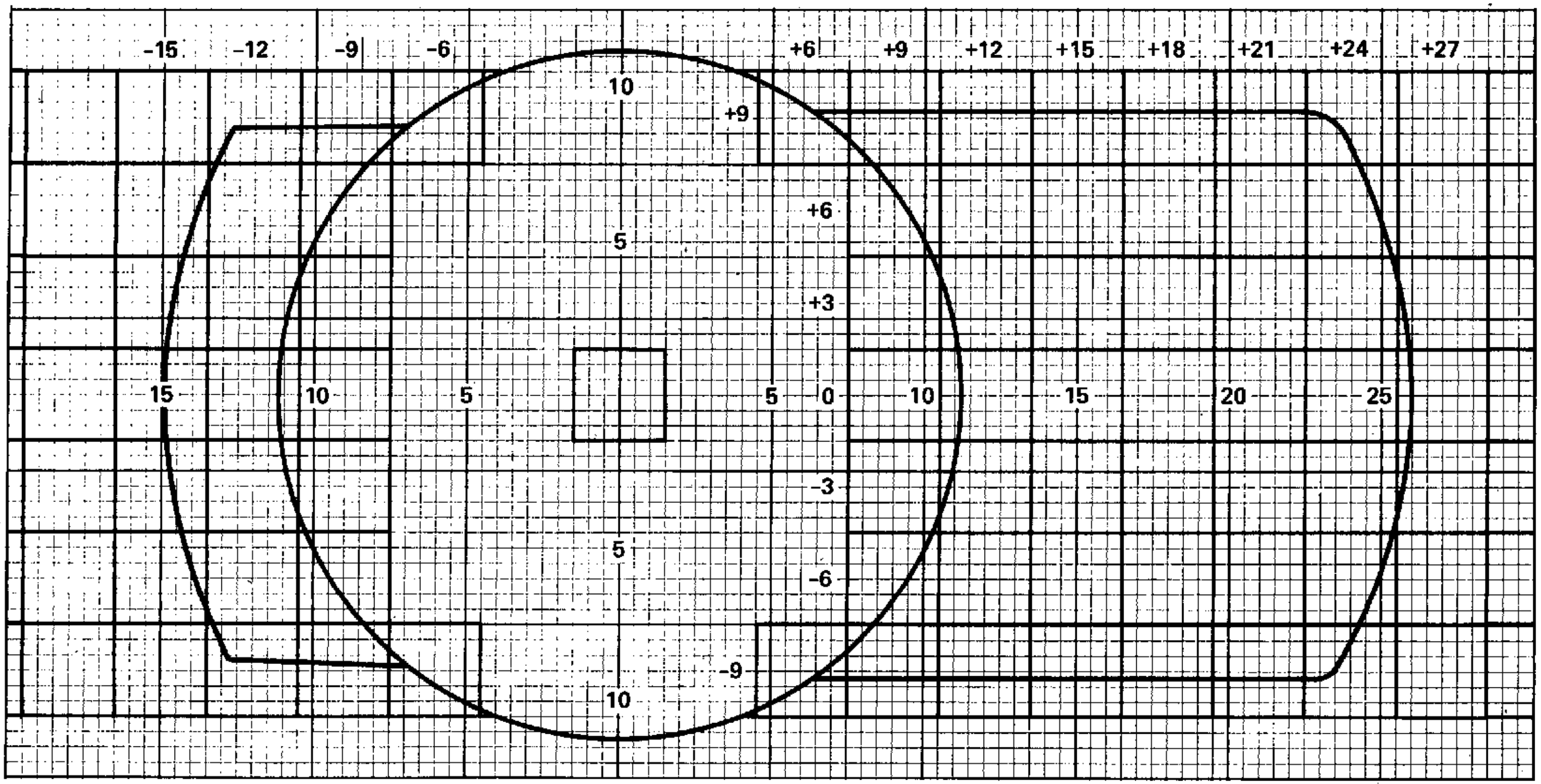

Figure 4. Scan Step 10

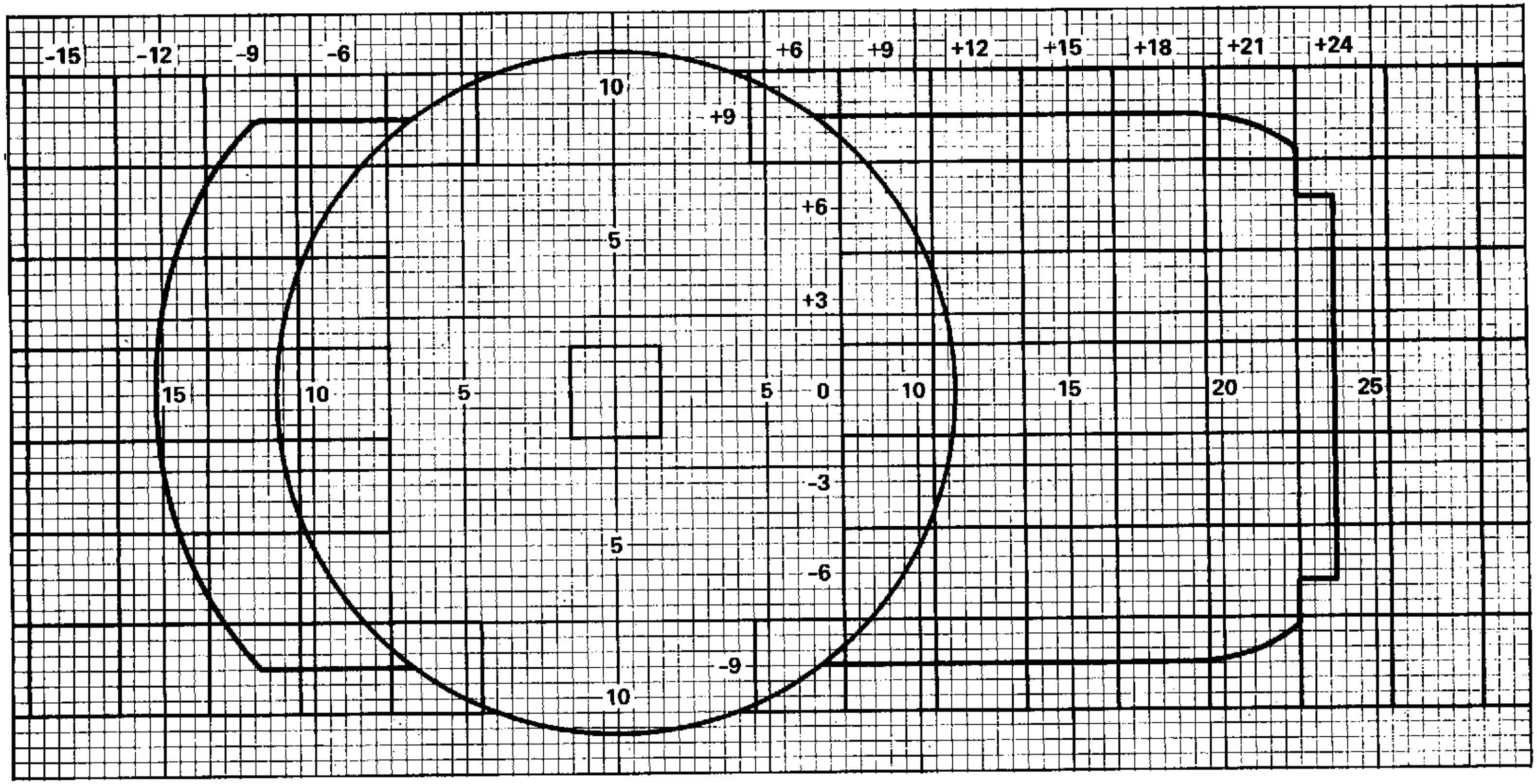

Figure 5. Scan Step 12

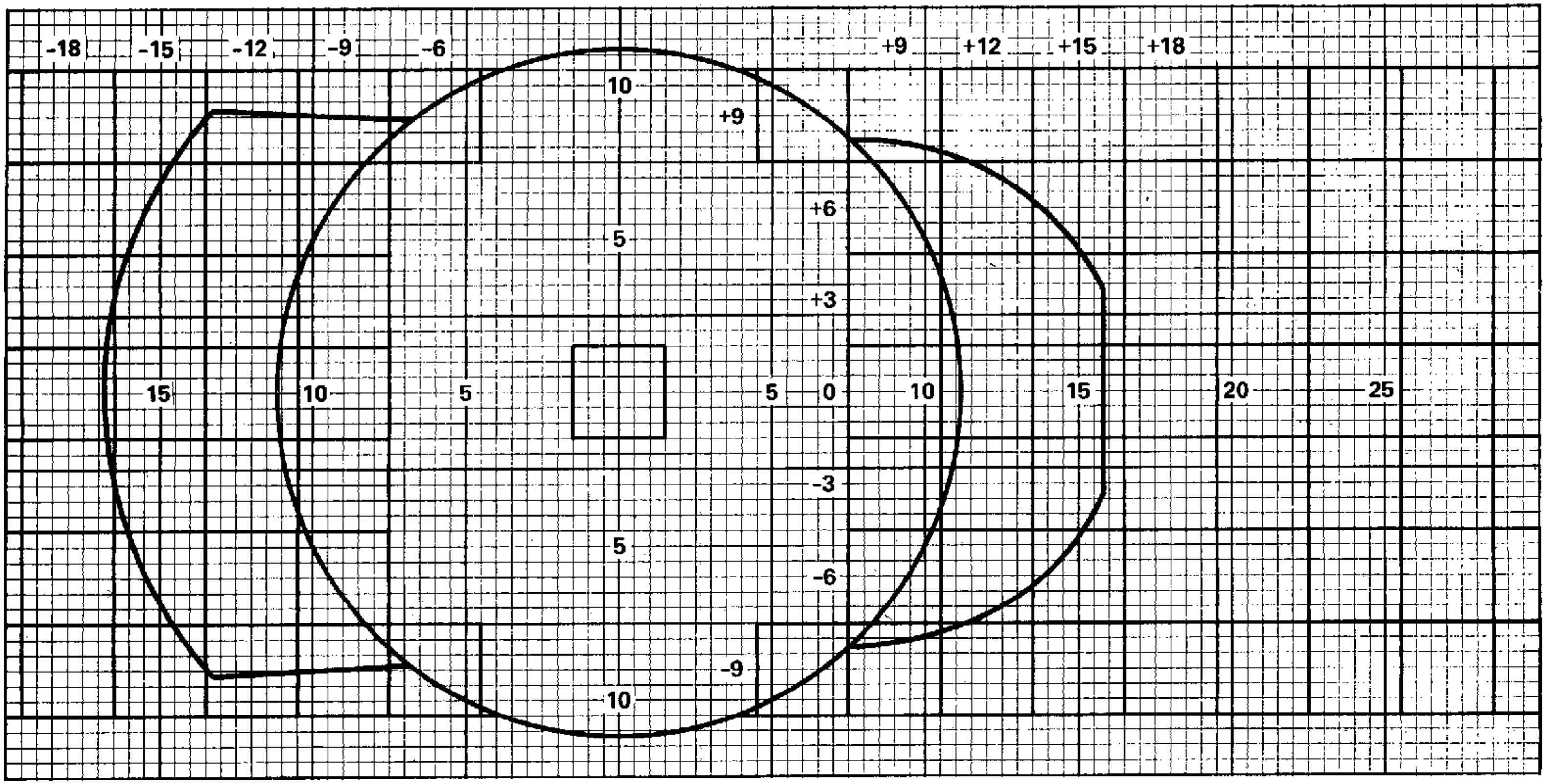

Figure 6. Scan Step 18

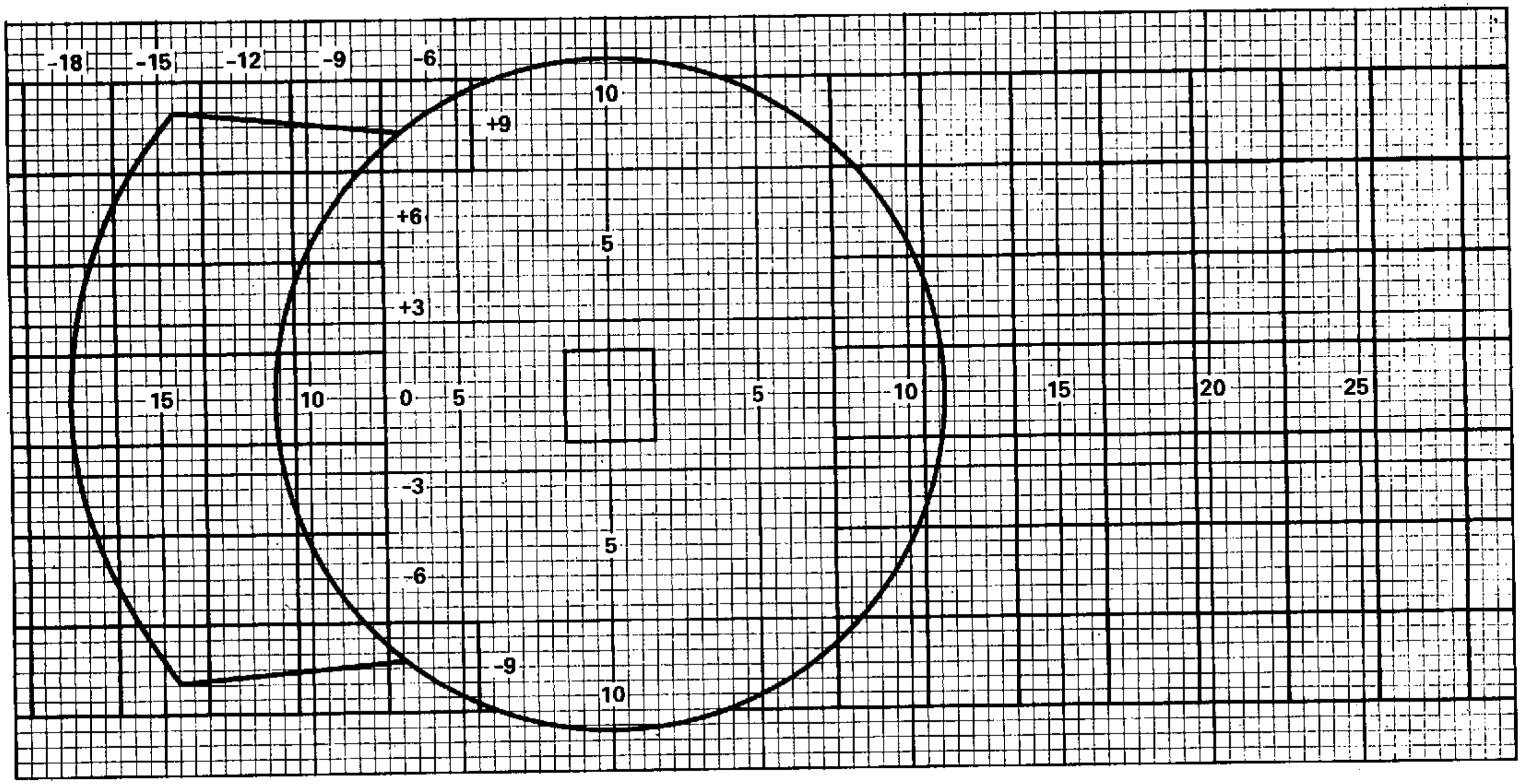

Figure 7. Scan Step 23

Table 2

FOV VTPR S/N 007 833 cm^{-1} Channel Scan Step 1

A_1 = 22.15 A_{1A} = 16.71 = NO. OF ELEMENTS USED FOR OBTAINING V_1

	-18°	-15°	-12°	-9°	-6°		+6°	+9°	+12°	+15°	+18°	+21°	+24°	+27°
							0.01	0.47	0.53	0.64	0.67	0.04		
						+9°								
								0.36	1 X	1 X	1 X	0.33 X		
						+6°			15.5=	27.5=	24.5=	22=		
									15.5	27.5	24.5	7.26		
									0.9 X	1 X	1 X	0.49 X		
						+3°			18=	42.5=	32.5=	24.5=		
									16.2	42.5	32.5	12.01		
									0.75 X	1 X	1 X	0.52 X		
						0°			13.5=	37.5=	26.5=	19.5=		
									10.13	37.5	26.5	10.14		
									0.9 X	1 X	1 X	0.49 X		
						-3°			15=	42.5=	32.5=	22.5=		
									13.5	42.5	32.5	11.03		
								0.36	1 X	1 X	1 X	0.33 X		
						-6°			18.5=	30.5=	24.5=	21.5=		
									18.5	30.5	24.5	7.10		
							0.01	0.47	0.53	0.64	0.67	0.04		
						-9°								
SUBTOTAL									73.83	180.5	140.5	47.54		

TOTAL: 442.37 $V_1 = \frac{442.37}{16.71}$ = 26.47 MV = AVE. VOLT. FOR STEP 1

NOTE: ELEMENTS MARKED WITH AN X NOT USED FOR OBTAINING V_1

Table 3

FOV VTPR S/N 007 Scan Step 6

$A_6 = 33.46$

	-18°	-15°	-12°	-9°	-6°
+9°				0.11 X	
				20.5=	
				2.26	
+6°			0.75 X	0.36	
			25=		
			18.75		
+3°			0.86 X		
			22=		
			18.92		
0°			0.74 X		
			20.5=		
			15.17		
-3°			0.86 X		
			19.5=		
			16.77		
-6°			0.75 X	0.36	
			25=		
			18.75		
-9°				0.11 X	
				19.5=	
				2.15	
SUBTOTAL			95.14	4.41	

$A_{6A} = 25.99$

	+6°	+9°	+12°	+15°	+18°	+21°	+24°	+27°
+9°	0.02	0.47	0.55	0.61	0.67	0.68	0.014	
+6°		0.36	1 X	1 X	1 X	1 X	0.3 X	
			15.5=	27.5=	24.5=	22=	17.5=	
			15.5	27.5	24.5	22	5.25	
+3°			0.9 X	1 X	1 X	1 X	0.53 X	
			18=	42.5=	32.5=	24.5=	10.5=	
			16.2	42.5	32.5	24.5	5.57	
0°			0.75 X	1 X	1 X	1 X	0.6 X	
			13.5=	37.5=	26.5=	19.5=	7=	
			10.13	37.5	26.5	19.5	4.2	
-3°			0.9 X	1 X	1 X	1 X	0.53 X	
			15=	42.5=	32.5=	22.5=	16=	
			13.5	42.5	32.5	22.5	8.48	
-6°		0.36	1 X	1 X	1 X	1 X	0.3 X	
			18.5=	30.5=	24.5=	21.5=	18=	
			18.5	30.5	24.5	21.5	5.4	
-9°	0.02	0.47	0.55	0.61	0.67	0.68	0.014	
SUBTOTAL			73.83	180.5	140.5	110.0	28.9	

TOTAL: 633.28

$V_6 = \frac{633.28}{25.99} = 24.35 \text{ MV}$

Table 4

FOV VTPR S/N 007 Scan Step 10

A_{10} = 39.59 A_{10A} = 31.53

	-18°	-15°	-12°	-9°	-6°	+6°	+9°	+12°	+15°	+18°	+21°	+24°	+27°
+9°			0.32 X	0.36 X	0.01	0.06	0.53	0.55	0.56	0.57	0.58	0.23	
			23=	20.5=									
			7.36	7.38									
+6°		0.14 X	0.99 X	0.36			0.36	1 X	1 X	1 X	1 X	0.78 X	
		41=	25=					15.5=	27.5=	24.5=	22=	17.5=	
		5.74	24.75					15.5	27.5	24.5	22	13.65	
+3°		0.39 X	0.9 X					0.9 X	1 X	1 X	1 X	0.99 X	0.05
		44=	22=					18=	42.5=	32.5=	24.5=	10.5=	
		17.16	19.8					16.2	42.5	32.5	24.5	10.40	
0°		0.49 X	0.75 X					0.75 X	1 X	1 X	1 X	1 X	0.16
		44=	20.5=					13.5=	37.5=	26.5=	19.5=	7=	
		21.56	15.38					10.13	37.5	26.5	19.5	7	
-3°		0.39 X	0.9 X					0.9 X	1 X	1 X	1 X	0.99 X	0.05
		39=	19.5					15=	42.5=	32.5=	22.5=	16=	
		15.21	17.55					13.5	42.5	32.5	22.5	15.84	
-6°		0.14 X	0.99 X	0.36			0.36	1 X	1 X	1 X	1 X	0.78 X	
		28=	25=					18.5=	30.5=	24.5=	21.5=	18=	
		3.92	24.75					18.5	30.5	24.5	21.5	14.04	
-9°			0.32 X	0.36 X	0.01	0.06	0.53	0.55	0.56	0.57	0.58	0.23	
			36=	19.5=									
			11.52	7.02									
SUBTOTAL		63.59	121.11	14.4				73.83	180.5	140.5	110.0	60.93	

TOTAL: 764.86

$$V_{10} = \frac{764.86}{31.53} = 24.26 \text{ MV}$$

Table 5

FOV VTPR S/N 007 Scan Step 12

$A_{12} = 35.54$ $A_{12A} = 29.26$

	-18°	-15°	-12°	-9°	-6°		+6°	+9°	+12°	+15°	+18°	+21°	+24°	+27°
			0.32 X	0.47 X	0.03		0.03	0.47	0.50	0.50	0.50	0.36		
			23=	20.5=		+9°								
			7.36	9.64										
		0.15 X	0.99 X	0.36				0.36	1 X	1 X	1 X	1 X	0.25 X	
		41=	25=			+6°			15.5=	27.5=	24.5=	22=	17.5=	
		6.15	24.75						15.5	27.5	24.5	22	4.38	
		0.47 X	0.9 X						0.9 X	1 X	1 X	1 X	0.42 X	
		44=	22=			+3°			18=	42.5=	32.5=	24.5=	10.5=	
		20.68	19.8						16.2	42.5	32.5	24.5	4.41	
		0.6 X	0.75 X						0.75 X	1 X	1 X	1 X	0.42 X	
		44=	20.5=			0°			13.5=	37.5=	26.5=	19.5=	7=	
		26.4	15.38						10.13	37.5	26.5	19.5	2.94	
		0.47 X	0.9 X						0.9 X	1 X	1 X	1 X	0.42 X	
		39=	19.5=			-3°			15=	42.5=	32.5=	22.5=	16=	
		18.33	17.55						13.5	42.5	32.5	22.5	6.72	
		0.15 X	0.99 X	0.36				0.36	1 X	1 X	1 X	1 X	0.25 X	
		28=	25=			-6°			18.5=	30.5=	24.5=	21.5=	18=	
		4.2	24.75						18.5	30.5	24.5	21.5	4.5	
			0.32 X	0.47 X	0.03		0.03	0.47	0.50	0.50	0.50	0.36		
			36=	19.5=		-9°								
			11.52	9.17										
SUBTOTAL		75.76	121.11	18.81					73.83	180.5	140.5	110.0	22.92	

TOTAL: 743.43

$$V_{12} = \frac{743.43}{29.26} = 25.41 \text{ MV}$$

Table 6

FOV VTPR S/N 007 Scan Step 18

$A_{18} = 20.02$ $\qquad$ $A_{18A} = 18.10$

	-18°	-15°	-12°	-9°	-6°		+6°	+9°	+12°	+15°	+18°	+21°	+24°	+27°
		0.12 X 25.5= 3.06	0.52 X 23= 11.96	0.47 X 20.5= 9.64	0.02	+9°								
		0.7 X 41= 28.7	1 X 25= 25	0.36		+6°		0.36	0.87 X 15.5= 13.49	0.16 X 27.5= 4.4				
		0.98 X 44= 43.12	0.9 X 22= 19.8			+3°			0.9 X 18= 16.2	0.74 X 42.5= 31.45				
	0.08 X 33= 2.64	1 X 44= 44	0.75 X 20.5= 15.38			0°			0.75 X 13.5= 10.13	0.8 X 37.5= 30.0				
		0.98 X 39= 38.22	0.9 X 19.5= 17.55			-3°			0.9 X 15= 13.5	0.74 X 42.5= 31.45				
		0.7 X 28= 19.6	1 X 25= 25	0.36		-6°		0.36	0.87 X 18.5= 16.10	0.16 X 30.5= 4.88				
		0.12 X 32= 3.84	0.52 X 36= 18.72	0.47 X 19.5= 9.17	0.02	-9°								
SUBTOTAL	2.64	180.54	133.41	18.81					69.42	102.18				

TOTAL: 507.0

$$V_{18} = \frac{507.0}{18.1} = 28.01 \text{ MV}$$

Table 7

FOV VTPR S/N 007 Scan Step 23

A_{23} = 14.38

	-18°	-15°	-12°	-9°	-6°	
		0.32 X 25.5= 8.16	0.58 X 23= 13.34	0.47 X 20.5= 9.64	0.01	+9°
	0.08 X 38= 3.04	0.97 X 41= 39.77	1 X 25= 25	0.36		+6°
	0.38 X 30= 11.4	1 X 44= 44	0.9 X 22= 19.8			+3°
	0.49 X 33= 16.17	1 X 44= 44	0.75 X 20.5= 15.38			0°
	0.38 X 28.5= 10.83	1 X 39= 39	0.9 X 19.5= 17.55			-3°
	0.08 X 27.5= 2.2	0.97 X 28= 27.16	1 X 25= 25	0.36		-6°
		0.32 X 32= 10.24	0.58 X 36= 20.88	0.47 X 19.5= 9.17	0.01	-9°
SUBTOTAL	43.64	212.33	136.95	18.81		

TOTAL: 411.73

A_{23A} = 13.64

+6°	+9°	+12°	+15°	+18°	+21°	+24°	+27°

$$V_{23} = \frac{411.73}{13.64} = 30.19 \text{ MV}$$

amount of the elemental area that lies within the far field of view. The second entry is the measured signal in millivolts (less noise voltage) and the third entry is the product of the first two entries. Elements that lie within the far field view but were not used for obtaining the average signal voltage contain one entry only (the portion of the elemental area within the far field view). Only those measurements that were made with a completely unobscured source were used. Two types of FOV measurements were made. The left side measurements were made using a large auxiliary flat mirror inserted between the scan and secondary mirrors. This gave good readings for the left side, but the secondary mirror obstructed most of the far field view on the right side. The right side readings that were used in the calculations were made with the scan mirror in the scan step 10 position (without the auxiliary mirror). The sum of the first entries is the value of A_n.

Bias Variation Tests

Two independent bias variation tests were made with S/N 007 without baffles. In the first test the average peak signal in the 833 cm^{-1} channel was 833.35 counts at scan step 9 (for scan step 10 the average signal was 833.1 counts). In the second test the average peak signal was 840.55 counts at scan step 10 (at step 9 the average signal was 840.45 counts). The average peak signal for both tests is 837 counts. The average readings for both tests are shown in Table 8.

Table 8

Bias Variation Tests Without Baffle (833 cm^{-1} Channel). Space Target $\approx$ 100 K.

Scan Step	Counts	
	Test 1	Test 2
1	827.3	835.05
2	828.5	836.05
5	831.0	838.95
9	833.35	840.45
10	833.1	840.55
12	831.5	839.83
15	830.75	837.8
19	826.8	834.2
22	823.2	831.45
23	823.4	831.70

Out-of-Focus Corrections

The need for extremely high signal-to-noise ratios necessitated the use of an uncollimated 2-inch diameter source at a distance of only 76 inches. Because of this, signal energy is lost due to (1) increase in obscuration of the secondary mirror, (2) decrease in the angular size of the telescope entrance pupil, and (3) out-of-focus blurring of the image.

1. Secondary Mirror Obscuration

   The shadow of the secondary mirror on the primary is increased when the source is moved from infinity to 76 inches. For a source at infinity the obscuration diameter is 1.125 inches. Since the back rim of the secondary is located 2.377 inches from the vertex of the primary, which has a 7.268-inch radius of curvature, the obscuration diameter is 1.161 inches (see Appendix 1).

2. Entrance Pupil Size

   For an on-axis point source at infinity the entrance pupil diameter is 2.970 inches. For a source at 76 inches the pupil diameter is 2.720 inches (see Appendix 2).

   The correction factor due to the change in angular size of both the primary and secondary mirrors is

$$\frac{(2.720)^2 - (1.161)^2}{(2.970)^2 - (1.125)^2} = 0.801$$

3. Out-of-Focus Blur

   The image of every source point is blurred by an angular diameter θ_B given by (see Appendix 2 for more precise calculation)

$$\theta_B \approx \frac{D}{S}$$

   where D = effective entrance pupil diameter
   S = distance of source from primary mirror

$$\therefore \theta_B \approx \frac{2.720}{76} = 0.0358 \text{ radian}$$

$$\approx 2.05^\circ$$

This blur size should be compared to the in-focus image size of 1.5° and the nominal 2.1° FOV of the VTPR. Because of this large blur the detector collects only 75.3% of the energy from the source, compared to what it would receive from an in-focus source. See Appendix 3 for detailed analysis of this energy loss.

The total correction factor is therefore

$$L = (0.801)(0.753) = 0.603$$

The optical system of the VTPR is summarized in Appendix 4.

APPENDIX 1

SECONDARY MIRROR OBSCURATION

APPENDIX 1

SECONDARY MIRROR OBSCURATION

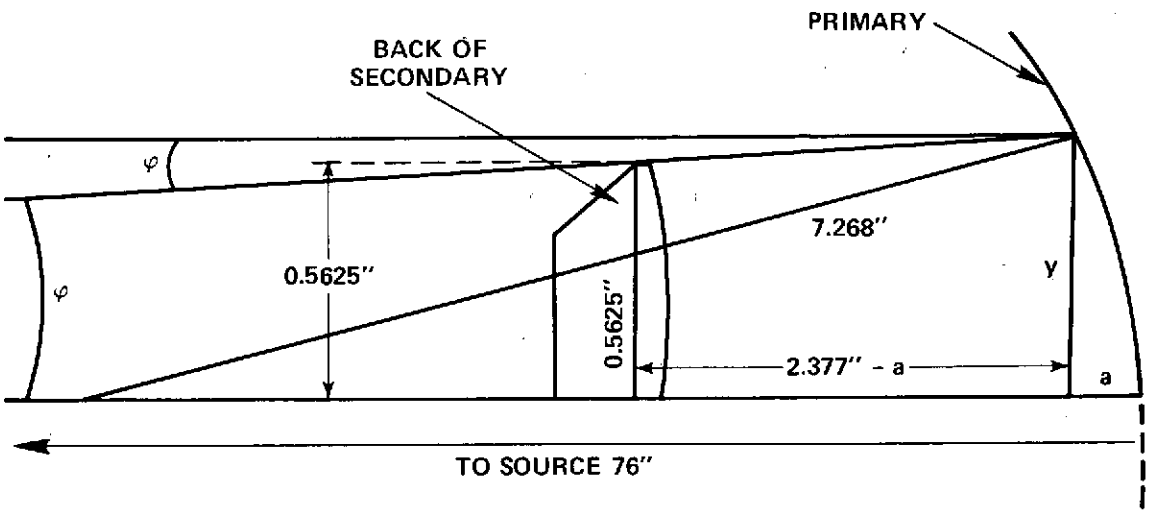

NOTE: NOT DRAWN TO SCALE

y = radius of circular shadow on primary

Primary radius of curvature = 7.268 inches

Secondary obscuration radius = 0.5625 inch

$$\tan\varphi = \frac{0.5625}{76 - 2.377} = 0.0076403$$

φ = 0.0076401 radian = 0.4378°
= subtended angle at source

$$y = (76 - a)\tan\varphi \qquad (1)$$

$$y^2 = (7.268)^2 - (7.268 - a)^2 \qquad (2)$$

Solving Equations 1 and 2 we get

y = 0.5807 inch
a = 0.0232 inch

The secondary obscuration diameter is therefore 1.161 inches.

APPENDIX 2

ENTRANCE PUPIL SIZE

APPENDIX 2

ENTRANCE PUPIL SIZE

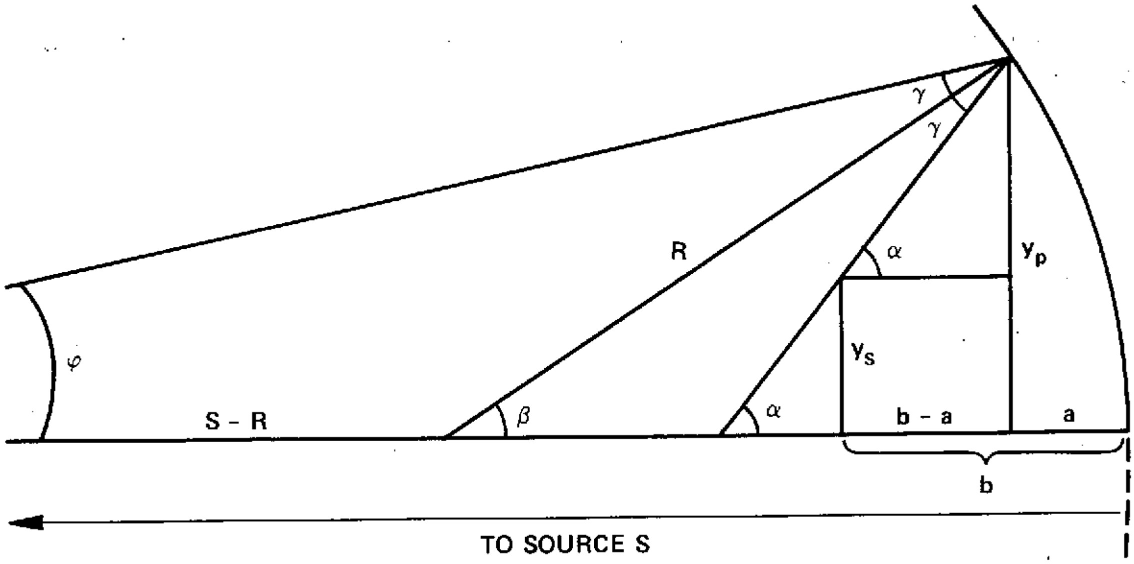

NOTE: NOT DRAWN TO SCALE

y_S = clear aperture radius of secondary = 0.540 inch

y_P = entrance pupil radius for point source at a distance S (on-axis)

R = radius of curvature of primary = 7.268 inches

b = distance of front of secondary mirror from vertex of primary = 2.317 inches

S = distance of source to primary vertex = 76 inches

$$a + \sqrt{R^2 - y_P^2} = R \tag{1}$$

$$\tan\alpha = \frac{y_P - y_S}{b - a} \tag{2}$$

$$\sin\beta = \frac{y_P}{R} \tag{3}$$

$$\gamma = \alpha - \beta \tag{4}$$

$$\varphi = \alpha - 2\gamma = 2\beta - \alpha \quad (5)$$

$$\frac{S - R}{\sin \gamma} = \frac{R}{\sin \varphi} \quad (6)$$

For y_S = 0.540 inch, R = 7.268 inches, b = 2.317 inches and S = 76 inches, the solution of the above six equations is

α = 0.35848 rad
β = 0.18823 rad
γ = 0.170245 rad
φ = 0.01798 rad
a = 0.1284 inch
y_P = 1.360 inches

The entrance pupil diameter for a source at 76 inches is therefore 2.720 inches. The angular radius of the entrance pupil is given by φ (0.01798 radian = 1.0302°).

APPENDIX 3

ENERGY LOSS DUE TO OUT-OF-FOCUS BLUR OF IMAGE

APPENDIX 3

ENERGY LOSS DUE TO OUT-OF-FOCUS BLUR OF IMAGE

The energy falling on the detector was found by convolving the image blur annulus with the square field-of-view of the detector. The annular shape is due to the image of the circular primary mirror obscured by the circular secondary mirror. The convolution was averaged along three paths,

1. horizontally through the center of the detector's nominal FOV (along the x-axis)
2. diagonally across the square FOV (at an angle of 45° with the x-axis)
3. at an angle of 22.5° with the x-axis

The results of the calculations are shown below.

δ (degrees)	0	22.5	45
p	0.7773	0.7615	0.7213

δ is the convolution path angle with respect to the x-axis and p is the relative energy falling on the detector. The average value for the three paths is 0.753.

The calculation details are described below.

1. Horizontal Convolution Path

   Along this path the convolution is divided into three parts where

   a. portions of both primary and secondary images lie outside the nominal FOV

   b. only the primary mirror image extends beyond the nominal FOV

   c. both primary and secondary images lie inside the nominal FOV.

   The following symbols and values will be used for all convolution paths

   r = angular radius of secondary mirror = 0.4378° (see Appendix 1)

   R = angular radius of primary mirror = 1.0302° (see Appendix 2)

   ρ = angular radius of in-focus image = $\tan^{-1} 1/76 = 0.7538°$

2α = angular, in-focus length of one side of the square field-of-view
$= 2.1° \ (\alpha = 1.05°)$

a. $\alpha - \rho \leqslant x \leqslant r$

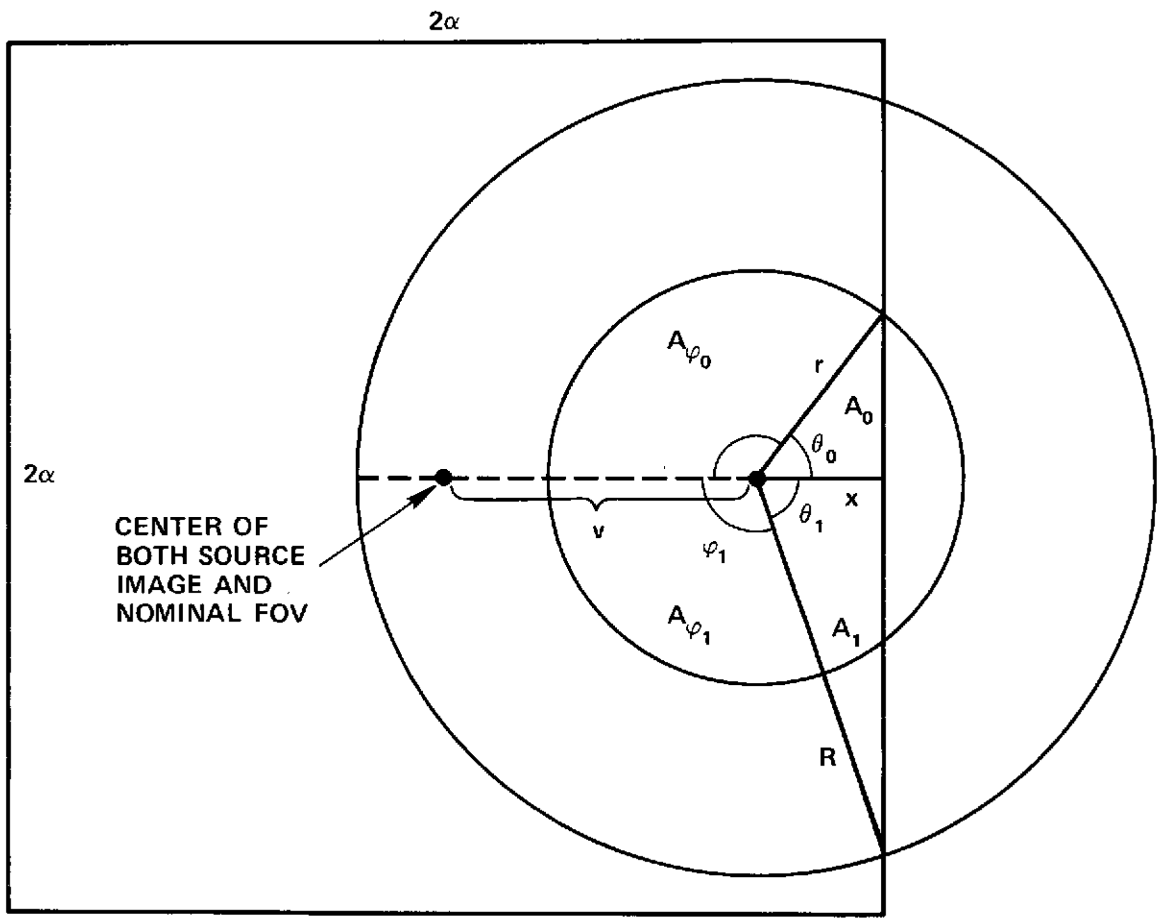

The point shown at an angular distance x from the side of the nominal FOV lies within the in-focus image of radius ρ.

If p_x is the relative image blur area that lies inside the square FOV for an in-focus image point at x then

$$p_{x1} = \frac{2(A_1 - A_0) + 2(A_{\phi_1} - A_{\phi_0})}{A_R - A_r}$$

where A_0 and A_1 are the triangular areas shown in the figure; $A\phi_0$ and $A\phi_1$ are the areas of the sectors shown; A_R is the area of the large circle (radius R) and A_r is the area of the small circle (radius r).

$$2A_0 = x\sqrt{r^2 - x^2}$$

$$2A_1 = x\sqrt{R^2 - x^2}$$

$$2A\phi_0 = \phi_0 r^2$$

$$2A\phi_1 = \phi_1 R^2$$

$$\theta_0 = \cos^{-1} \frac{x}{r}$$

$$\theta_1 = \cos^{-1} \frac{x}{R}$$

$$\phi_0 = \pi - \theta_0$$

$$\phi_1 = \pi - \theta_1$$

$$p_{x1} = \frac{x\sqrt{R^2 - x^2} - x\sqrt{r^2 - x^2} + (\pi - \theta_1) R^2 - (\pi - \theta_0) r^2}{\pi (R^2 - r^2)}$$

b. $r \leqslant x \leqslant R$

$$p_{x2} = \frac{x\sqrt{R^2 - x^2} + (\pi - \theta_1) R^2 - \pi r^2}{\pi (R^2 - r^2)}$$

c. $R \leqslant x \leqslant \alpha$

$$p_{x3} = 1$$

Since there is more energy from a circular ring toward the edge of the source than toward the center the total energy falling on the detector must be weighted accordingly. If v is the (angular) distance of the in-focus image point from the center of the image of the source the total integrated relative energy p received by the detector is

$$p = \int_0^{\rho} \frac{2\pi v}{\pi \rho^2} p_x \, dv = \frac{2}{\rho^2} \int_0^{\rho} v p_x \, dv$$

Since

$$v = \alpha - x$$

$$dv = -dx$$

$$p = -\frac{2}{\rho^2}\int_{\alpha}^{\alpha-\rho} (\alpha - x)\, p_x\, dx = \frac{2}{\rho^2}\int_{\alpha-\rho}^{\alpha} (\alpha - x)\, p_x\, dx$$

$$= \frac{2}{\rho^2}\int_{\alpha-\rho}^{r} (\alpha - x)\, p_{x1}\, dx + \frac{2}{\rho^2}\int_{r}^{R} (\alpha - x)\, p_{x2}\, dx$$

$$+ \frac{2}{\rho^2}\int_{R}^{\alpha} (\alpha - x)\, dx$$

Let

$$I_1 = \frac{2}{\rho^2}\int_{\alpha-\rho}^{r} (\alpha - x)\, p_{x1}\, dx$$

$$= \frac{2}{\rho^2}\int_{0.2962}^{0.4378} (\alpha - x)\, p_{x1}\, dx$$

$$I_2 = \frac{2}{\rho^2}\int_{r}^{R} (\alpha - x)\, p_{x2}\, dx$$

$$= \frac{2}{\rho^2}\int_{0.4378}^{1.0302} (\alpha - x)\, p_{x2}\, dx$$

$$I_3 = \frac{2}{\rho^2}\int_{R}^{\alpha} (\alpha - x)\, dx$$

$$= \frac{2}{\rho^2} \int_{1.0302}^{1.05} (\alpha - x)\, dx$$

$$= \frac{2}{(0.7538)^2} \left[\alpha x - \frac{x^2}{2} \right]_{1.0302}^{1.05}$$

$$= 0.0007$$

I_1 and I_2 were integrated numerically and the results are

$$I_1 = 0.2275$$

$$I_2 = 0.5491$$

$$p = I_1 + I_2 + I_3 = 0.7773$$

2. Diagonal Path

Along the diagonal the image of the secondary remains entirely within the square FOV of the detector. However, it is still necessary to consider the following three cases:

a. The image of the primary extends beyond the corner of the square FOV.

b. The image of the primary extends beyond the sides of the FOV but not the corner.

c. The entire image of the primary lies within the detector's FOV.

a. $\alpha - \frac{\rho}{\sqrt{2}} \leqslant x \leqslant \frac{R}{\sqrt{2}}$

$$p_{x1} = \frac{2(A_1 + A_0 + A_\phi) - \pi r^2}{\pi (R^2 - r^2)}$$

$$2A_1 = x\sqrt{R^2 - x^2}$$

$$2A_0 = x^2$$

$$2A_\phi = \phi R^2$$

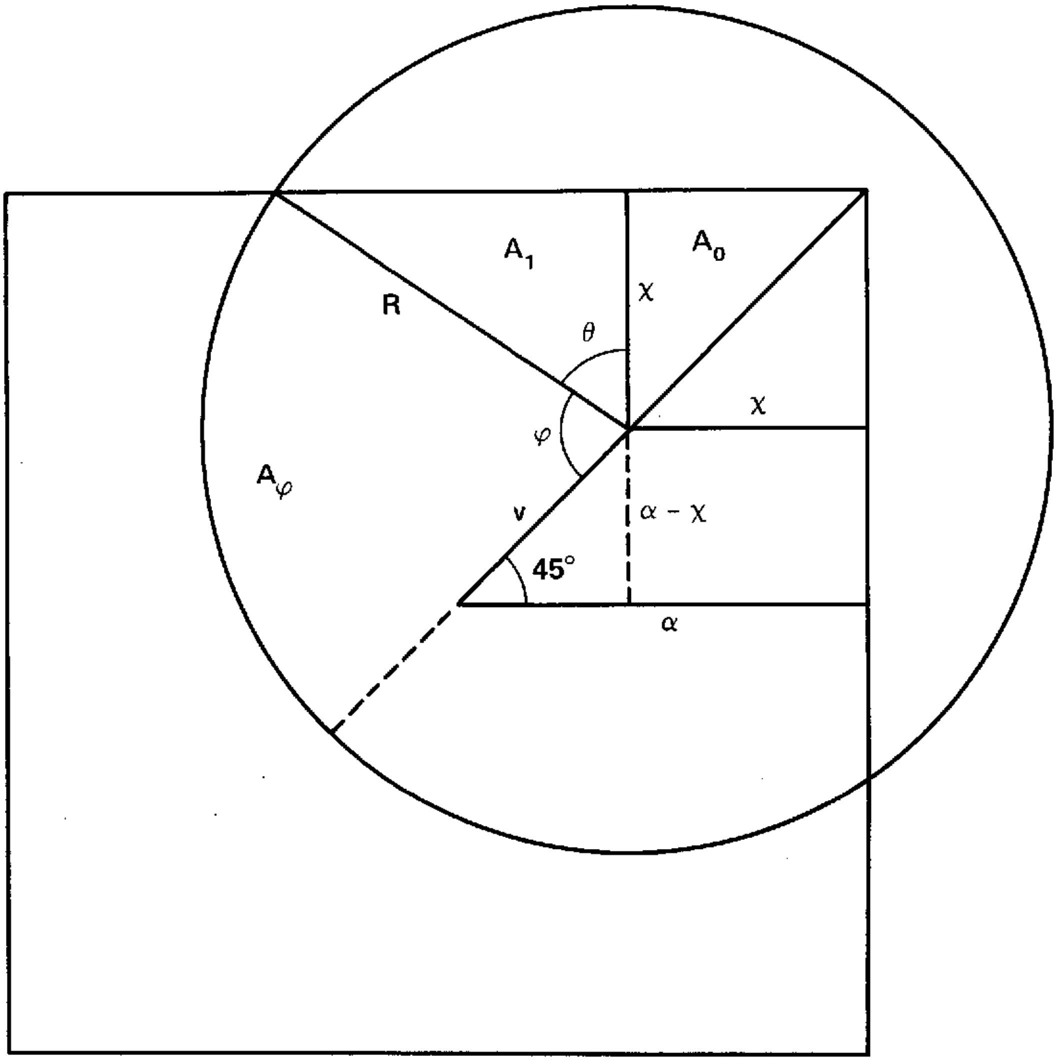

$$\phi = \frac{3\pi}{4} - \theta$$

$$\theta = \cos^{-1} \frac{x}{R}$$

$$\therefore p_{x1} = \frac{x\sqrt{R^2 - x^2} + x^2 + (3\pi/4 - \theta)\, R^2 - \pi r^2}{\pi\, (R^2 - r^2)}$$

b. $\frac{R}{\sqrt{2}} \leqslant x \leqslant R$

$$p_{x2} = \frac{2x\sqrt{R^2 - x^2} + (\pi - 2\theta)\, R^2 - \pi r^2}{\pi\, (R^2 - r^2)}$$

c. $R \leqslant x \leqslant \alpha$

$$p_{x3} = 1$$

The integrated energy along the diagonal is

$$p = \frac{2}{\rho^2} \int_0^{\rho} p_x \, v \, dv$$

For this case,

$$v = \sqrt{2}\,(\alpha - x)$$

$$dv = -\sqrt{2}\, dx$$

$$p = -\frac{4}{\rho^2} \int_{\alpha}^{\alpha - \frac{\rho}{\sqrt{2}}} p_x \,(\alpha - x)\, dx$$

$$= \frac{4}{\rho^2} \int_{\alpha - \frac{\rho}{\sqrt{2}}}^{\alpha} (\alpha - x)\, p_x \, dx$$

$$= \frac{4}{\rho^2} \int_{\alpha - \frac{\rho}{\sqrt{2}}}^{\frac{R}{\sqrt{2}}} (\alpha - x)\, p_{x1} \, dx + \frac{4}{\rho^2} \int_{\frac{R}{\sqrt{2}}}^{R} (\alpha - x)\, p_{x2} \, dx$$

$$+ \frac{4}{\rho^2} \int_{R}^{\alpha} (\alpha - x)\, dx$$

$$= I_1 + I_2 + I_3$$

$$I_1 = \frac{4}{\rho^2} \int_{\alpha - \frac{\rho}{\sqrt{2}}}^{\frac{R}{\sqrt{2}}} (\alpha - x)\, p_{x1} \, dx = \frac{4}{\rho^2} \int_{0.5170}^{0.7285} (\alpha - x)\, p_{x1} \, dx$$

$$I_2 = \frac{4}{\rho^2} \int_{\frac{R}{\sqrt{2}}}^{R} (\alpha - x)\, p_{x2}\, dx = \frac{4}{\rho^2} \int_{0.7285}^{1.0302} (\alpha - x)\, p_{x2}\, dx$$

$$I_3 = \frac{4}{\rho^2} \int_{R}^{\alpha} (\alpha - x)\, dx = \frac{4}{\rho^2} \int_{1.0302}^{1.05} (\alpha - x)\, dx$$

$$I_3 = \frac{4}{(0.7538)^2} \left| \alpha x - \frac{x^2}{2} \right|_{1.0302}^{1.05} = 0.0014$$

Numerical integration of I_1 and I_2 yields

$I_1 = 0.4179$

$I_2 = 0.3020$

$\therefore p = 0.7213$

3. Convolution Path Angle of 22.5°

Along this path five cases are considered.

a. The primary mirror image extends beyond the corner of the nominal FOV and the secondary mirror image extends beyond one side of the FOV.

b. Same as above except that the secondary mirror image lies entirely within the square FOV.

c. The primary mirror image extends beyond two sides of the square FOV but not beyond the corner.

d. The primary mirror image extends beyond only one side of the FOV.

e. The primary mirror image lies entirely within the FOV.

a. $\alpha - \rho \cos \delta \leqslant x \leqslant r$

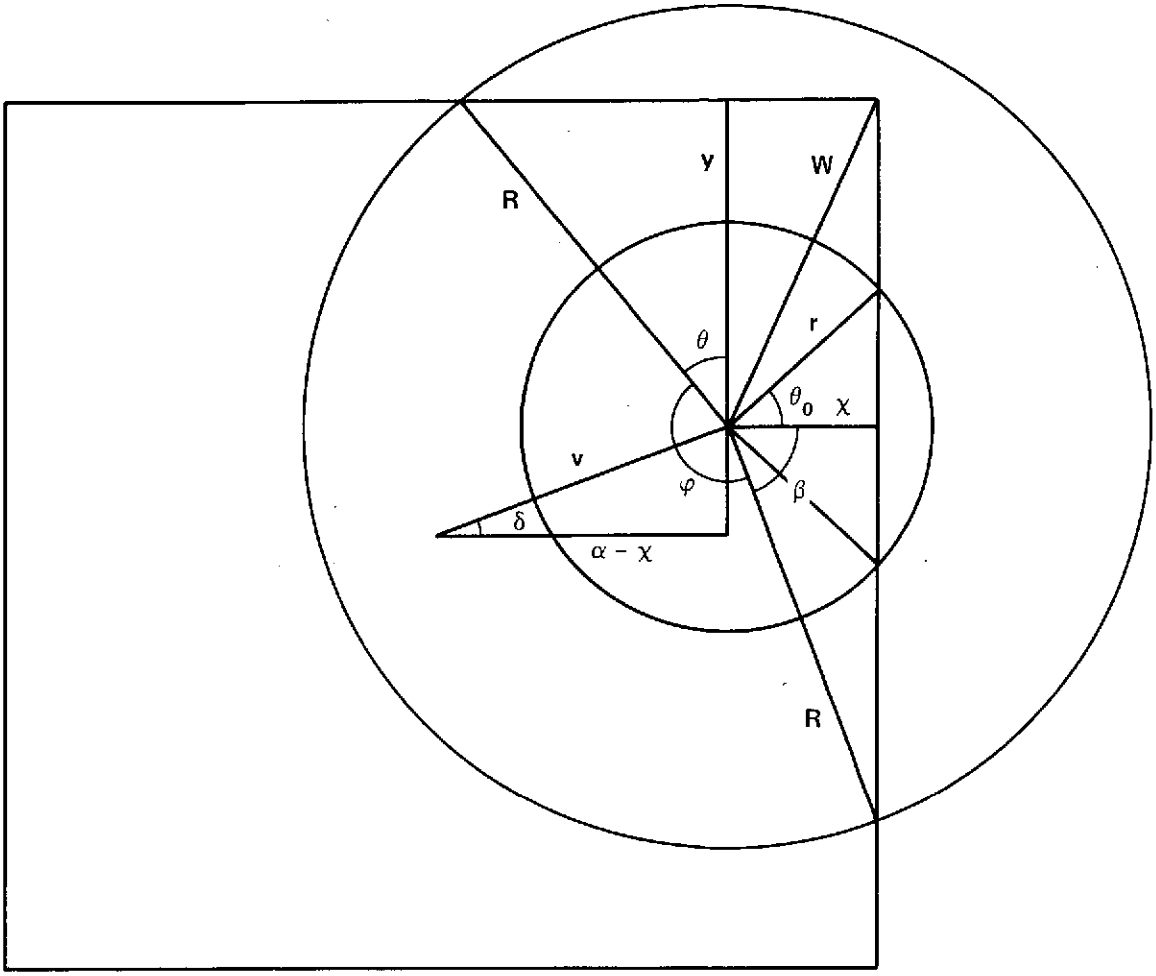

$$p_{x1} = \frac{y/2\sqrt{R^2 - y^2} + yx + x/2\sqrt{R^2 - x^2} + \phi/2\, R^2 - (\pi - \theta_0)\, r^2}{2.7321}$$

where

$$y = \alpha - (\alpha - x) \tan \delta$$

$$\phi = \frac{3\pi}{2} - (\theta + \beta)$$

$$\theta = \cos^{-1} \frac{y}{R}$$

$$\beta = \cos^{-1}\frac{x}{R}$$

$$\theta_0 = \cos^{-1}\frac{x}{r}$$

Note that $\pi(R^2 - r^2) = 2.7321$

b. $r \leqslant x \leqslant x_0$

x_0 is the value of x for which w (see preceding figure) is equal to R. x_0 can be found from the following equation:

$$w^2 = x^2 + y^2 = R^2 = x^2 + [\alpha - (\alpha - x)\tan\delta]^2$$

For $\delta = 22.5°$, $\alpha = 1.05$, $R = 1.0302$, the solution is

$$x_0 = 0.5764$$

$$p_{x2} = \frac{y/2\sqrt{R^2 - y^2} + yx + x/2\sqrt{R^2 - x^2} + \phi/2\, R^2 - \pi r^2}{2.7321}$$

c. $0.5764 \leqslant x \leqslant x_1$

x_1 is the value of x for which $y = R$. It can be found using the equation

$$y = R = \alpha - (\alpha - x)\tan\delta$$

For $\delta = 22.5°$, $\alpha = 1.05$, $R = 1.0302$

$$x_1 = 1.0022$$

$$p_{x3} = \frac{x\sqrt{R^2 - x^2} + y\sqrt{R^2 - y^2} + \phi/2\, R^2 + \gamma/2\, R^2 - \pi r^2}{2.7321}$$

where

$$\phi = \frac{3\pi}{2} - (\theta + \beta)$$

$$\gamma = \frac{\pi}{2} - (\theta + \beta)$$

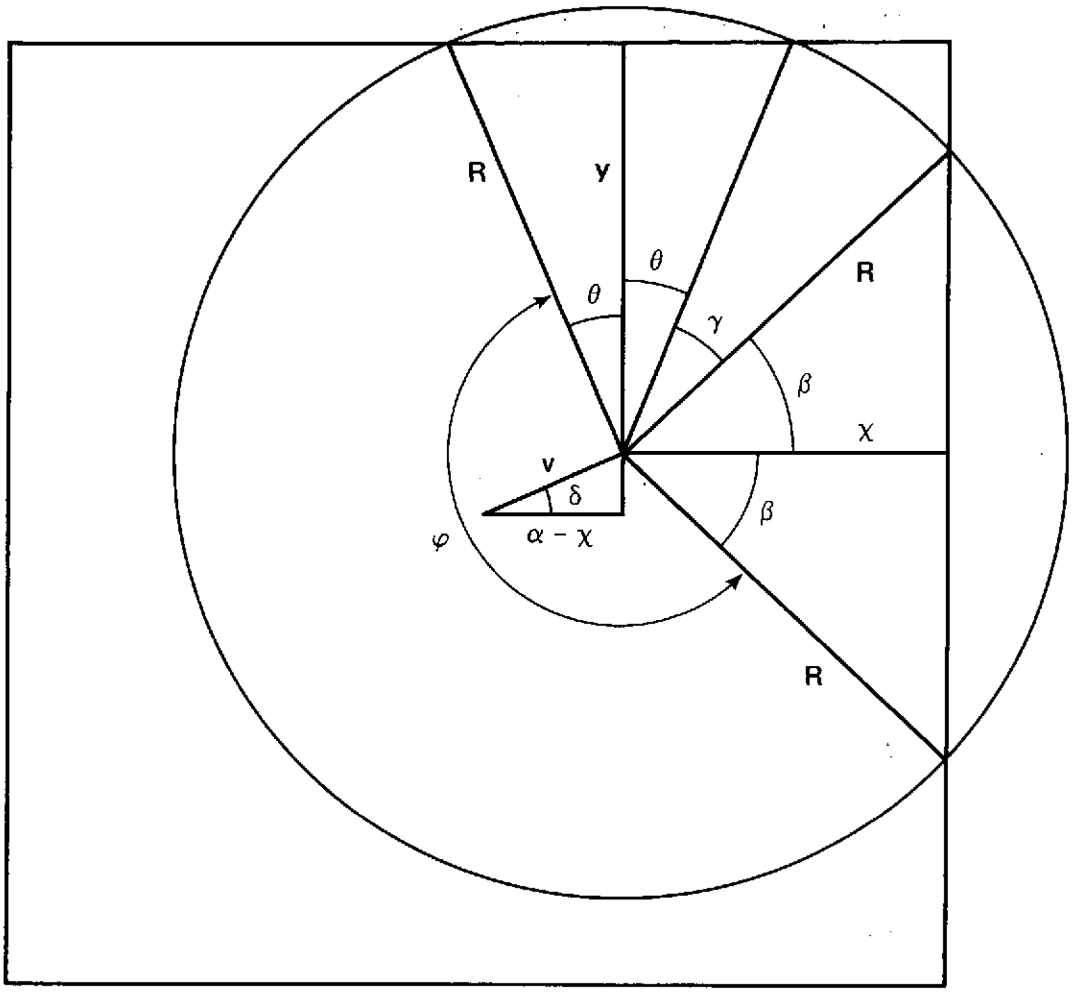

$$\therefore \frac{\phi}{2} R^2 + \frac{\gamma}{2} R^2 = (\pi - \theta - \beta) R^2$$

$$p_{x3} = \frac{x\sqrt{R^2 - x^2} + y\sqrt{R^2 - y^2} + (\pi - \theta - \beta) R^2 - \pi r^2}{2.7321}$$

d. $1.0022 \leqslant x \leqslant R$

$$p_{x4} = \frac{x\sqrt{R^2 - x^2} + (\pi - \beta) R^2 - \pi r^2}{2.7321}$$

e. $R \leqslant x \leqslant \alpha$

$$p_{x5} = 1$$

The integrated energy along δ is

$$p = \frac{2}{\rho^2} \int_0^{\rho} p_x \, dx$$

where now

$$v = \frac{\alpha - x}{\cos \delta}$$

$$dv = - \frac{dx}{\cos \delta}$$

$$p = \frac{2}{\rho^2 \cos^2 \delta} \int_{\alpha - \rho \cos \delta}^{\alpha} (\alpha - x) \, p_x \, dx$$

$$= \frac{2}{\rho^2 \cos^2 \delta} \int_{0.3535}^{0.4378} (\alpha - x) \, p_{x1} \, dx + \frac{2}{\rho^2 \cos^2 \delta} \int_{0.4378}^{0.5764} (\alpha - x) \, p_{x2} \, dx$$

$$+ \frac{2}{\rho^2 \cos^2 \delta} \int_{0.5764}^{1.0022} (\alpha - x) \, p_{x3} \, dx + \frac{2}{\rho^2 \cos^2 \delta} \int_{1.0022}^{1.0302} (\alpha - x) \, p_{x4} \, dx$$

$$+ \frac{2}{\rho^2 \cos^2 \delta} \int_{1.0302}^{1.05} (\alpha - x) \, dx$$

$$= I_1 + I_2 + I_3 + I_4 + I_5$$

For $\delta = 22.5°$,

$$I_1 = 4.1237 \int_{0.3535}^{0.4378} (\alpha - x) \, p_{x1} \, dx = 0.1490$$

$$I_2 = 4.1237 \int_{0.4378}^{0.5764} (\alpha - x) \, p_{x2} \, dx = 0.2148$$

$$I_3 = 4.1237 \int_{0.5764}^{1.0022} (\alpha - x)\, p_{x3}\, dx = 0.3930$$

$$I_4 = 4.1237 \int_{1.0022}^{1.0302} (\alpha - x)\, p_{x4}\, dx = 0.0039$$

$$I_5 = 4.1237 \int_{1.0302}^{1.05} (\alpha - x)\, dx = 0.0008$$

$$\therefore p = 0.7615$$

APPENDIX 4

SUMMARY OF VTPR OPTICAL SYSTEM

APPENDIX 4

SUMMARY OF VTPR OPTICAL SYSTEM

1. Primary Mirror

   Clear aperture diameter: 2.970 inches
   Radius of curvature: 7.268 inches
   Vertex thickness: 0.060 inches
   Hole diameter: 0.60 inches
   Distance of rim ray focus from vertex: 3.555 inches
   Effective focal length: 3.736 inches

2. Secondary Mirror

   Clear aperture diameter: 1.080 inches
   Obscuration diameter: 1.125 inches
   Radius of curvature: 4.886 inches
   Rim thickness: 0.060 inches
   Distance between primary and secondary: 2.317 inches (varied for best focus)

3. Telescope

   Effective focal length: 7.955 inches
   Distance between focus and back of primary: 0.465 inches
   Distance between focus and front of primary: 0.525 inches

4. Field stop size: 0.700 x 0.700 inches

   The optical layout is shown in the following figure.

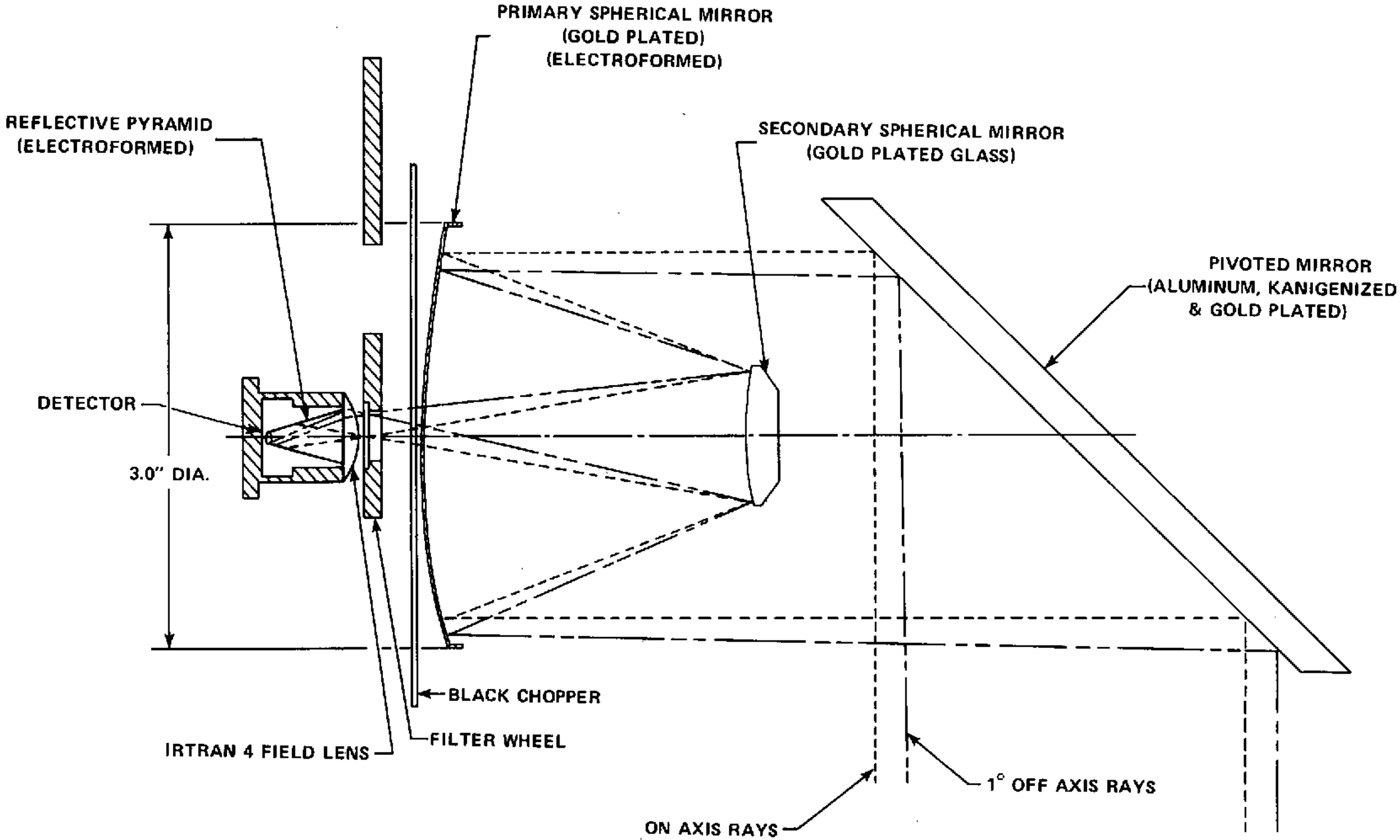

Optical Layout - VTPR